IIETA International Information and Engineering Technology Association
Advancing the World of Information and Engineering

International Journal of Heat and Technology
Vol. 43, No. 2, April, 2025, pp. 381-390
Journal homepage: http://iieta.org/journals/ijht

Magnetohydrodynamic Laminar Natural Convection in a Two-Dimensional Trapezoidal Porous Cavity Filled with Hybrid Nanofluid (Al_2O_3–Cu/Water) Flow: Entropy Generation

Mohamed A. Medebber[1*], Sahnoun Zeng[2], Noureddine Retiel[2]

[1] Mechanical Engineering Department, Mostapha Istambouli University, Mascara 29000, Algeria
[2] Mechanical Engineering Department, Abdelhamid Ibn Badis University, Mostaganem 27000, Algeria

Corresponding Author Email: m.medebber@univ-mascara.dz

https://doi.org/10.18280/ijht.430201

Received: 25 September 2024
Revised: 5 April 2025
Accepted: 19 April 2025
Available online: 30 April 2025

Keywords:
magnetohydrodynamic convection, Al_2O_3-water nanofluid, location of the inner obstacle cylinder

ABSTRACT

In the present study, the entropy generation of Magnetohydrodynamic free convection in a two dimensional trapezoidal enclosure filled with hybrid nanofluid Al_2O_3-Cu/water was numerically analyzed. The hybrid nanofluid flow is designated using the Brinkman-Forchheimer model. A finite volume approach is used to solve the Navier Stock equations numerically. A range of dimensionless variables, such as the Rayleigh number (Ra=10^4, 10^5, 10^6), the position of inner hot rectangular barrier (0.5, 1.0, 1.5) and Hartmann number (Ha=0, 25, 50, 100) were simulated numerically. The numerical results are illustrated in forms of streamlines, isotherms, entropy generation, and the average of Nusselt number. They indicated that the convective heat transfer becomes significant when (Ra) increases, while it decreases when (Ha) increases. Also, it is seen that the location of hot barrier affects significantly the entropy generation. Furthermore, it is demonstrated that the thermal and the dynamical behaviour of the hybrid nanofluid enhanced pattern degrades with strong Hartmann values, which significantly decreased the entropies generation. In order to improve heat transfer, it is recommended to reduce the magnetic influence.

1. INTRODUCTION

In recent years, a variety of engineering uses such as electrical parts cooling [1, 2], crystal formation, heat exchangers [3], and solar collectors [4, 5], have drawn a lot of attention to natural convection in closed cavities. Several important research works on natural convection in several cavities can be get in the previous studies [6-10]. Convective heat transfer in U-shaped enclosure has several scientific uses. and mechanical engineering. Esfe et al. [11] have investigated the free convection in a porous enclosure in a U shape contained Al_2O_3/H_2O nanofluid. They have used the two-phase mixture method. The results showed that the heat transfer rate and average Nusselt number increase with the increasing of the volume fraction of Al_2O_3 nanoparticles. Ali et al. [12] used the Galerkin finite element method to study the magnetohydrodynamic convection of a non-Newtonian nanofluid in a U-shaped enclosure. Nabwey et al. [13] investigated unsteady natural convection. They founded that the magnetic field control the heat transfer. In the last decade, we have seen a significant rise of nanofluids in industrial applications. The base fluid's thermal conductivity is raised by the nanoparticles. Choi and Eastman [14] investigated "nanofluids" used in engineering applications. Khanafer et al. [15] studied the natural convection in a closed cavity filled with nanofluid. They concluded that the heat transfer increase proportionally with increasing of volume fraction of nanoparticules. In addition, Khanafer and Vafai [16] experimentally investigated thermal conductivity models of nanofluid. Buongiorno [17] studied natural convection enhancement associated with using nanofluid. He founded a new analytical model for the transport phenomena in nanofluid. Kefayati [18] analyzed the two dimensional free convection and entropy generation in a porous square cavity filled with non-Newtonian nanofluid. They showed that the fluid friction changes with the power-law index for various numbers of Da. Al-Kouz et al. [19] analysed laminar natural convection in a tilted square enclosure equipped with hot walls. The free convection of Al_2O_3/H_2o nanofluid in a square enclosure under Lorenz force was investigated by Ghasemi et al. [20]. They showed that concentration of nanofluid enhance strongly the heat transfer for important Rayleigh number. Also, Kefayati et al. [21] used a lattice Boltzmann approach to investigate the natural convection's movement and heat transfer in square enclosure filled with water/SiO_2. They defined that there is a correlation ship between the Nusselt number, the volume fraction ϕ and Rayleigh number. Al-Kouz et al. [22] investigated the natural convection gas under low pressure inside a square cavity filled with of (Air/Al_2O_3) nanofluid.

Recently, many researches were produced to investigate the application of the magnetic nanofluids in porous enclosures. Recent research indicates that the use of hybrid nanofluids is crucial for engineering applications [23, 24]. The exploration of Nanoparticles' thermophysical properties and applications of the magnetic nanofluids in porous enclosures fascinated scientists. These nanoparticles are suspended in base fluids that have subpar thermophysical characteristics [25-27]. Moreover, the previous studies examined the addition of nanoparticles on the thermal conductivity [28, 29]. They discovered that even at modest volume fractions, nanoparticles can dramatically boost heat conductivity. In addition, the investigation of Acharya et al. [30] and Subhani and Nadeem [31] examined the causes of the increasing thermal conductivity, especially in magnetic fields and porous media. By assessing several hybrid nanofluids in the cavity, some researchers looked into how the type of nanoparticles affected heat transfer [32]. The utilization of hybrid nanofluid with important thermophysical properties improves heat transfer.

A few review papers re-examined the impact of hybrid nanofluid characteristics on the system's total generated entropy. It is important to remember that although these fluids' properties have a significant impact on heat transmission, they also promote irreversibilities [33-37]. They noted that the Lorenz force has a significant effect on the entropy generation.

Despite these advancements, the literature hasn't thoroughly examined the development of entropy in complex geometries filled with a hybrid nanofluid under a Lorenz force. This research examines the entropy generation of laminar convection flow in a trapezoidal enclosure filled with hybrid nanofluid under the influence of a magnetic field.

2. PHYSICAL AND MATHEMATICAL

Figure 1 shows a physical model of a two-dimensional trapezoidal cavity of height and width (L) geometric parameters. The liquid filled in the enclosure is a hybrid Al_2O_3-Cu/water (50/50) nanofluid. The horizontal walls of the enclosure are adiabatic, while the two vertically inclined walls are maintained at constant cold temperatures (T_C). The inner heated rectangular obstacle is minted at hot temperature T_H. The cavity is applied to a constant horizontal magnetic field (B). Also, the space medium of the cavity is a homogeneous porous material. It is supposed that the liquid is incompressible, Newtonian, the Boussinesq approximation is validated and the flow is laminar and steady.

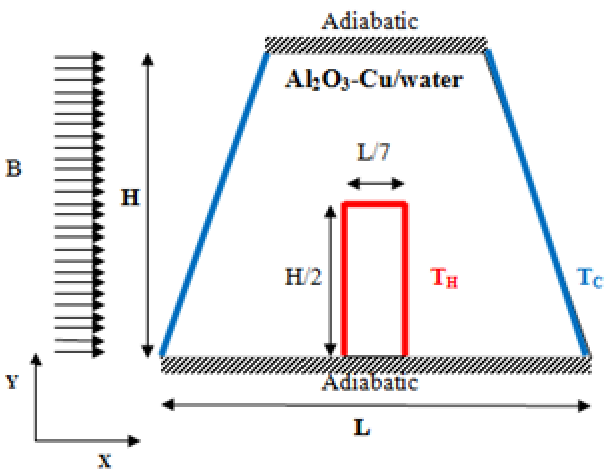

Figure 1. The physical model

2.1 Mathematical modeling

2.1.1 Governing equations and boundary

The Darcy-Brinkman-Forchheimer model is used to solve the Navier Stock equations, taking into account the Boussinesq approximation [23, 38, 39]:

$$\frac{\partial u}{\partial x}+\frac{\partial v}{\partial y}=0 \tag{1}$$

$$\frac{\rho_{nf}}{\epsilon^2}\left(u\frac{\partial u}{\partial x}+v\frac{\partial u}{\partial y}\right) = -\frac{1}{\rho_{nf}}\frac{\partial p}{\partial x}+\frac{\mu_{nf}}{\epsilon}\left(\frac{\partial^2 u}{\partial x^2}+\frac{\partial^2 u}{\partial y^2}\right) + -\frac{\mu_{nf}}{K}u - \frac{1.75\rho_{nf}}{\sqrt{150K}\epsilon^{\frac{3}{2}}}\left(\sqrt{u^2+v^2}\right)u \tag{2}$$

$$\frac{\rho_{nf}}{\epsilon^2}\left(u\frac{\partial v}{\partial x}+v\frac{\partial v}{\partial y}\right) = -\frac{1}{\rho_{nf}}\frac{\partial p}{\partial y}+\frac{\mu_{nf}}{\epsilon}\left(\frac{\partial^2 v}{\partial x^2}+\frac{\partial^2 v}{\partial y^2}\right) + (\rho\beta)_{nf}g(T-T_c) - \frac{\mu_{nf}}{K}v - \frac{1.75\rho_{nf}}{\sqrt{150K}\epsilon^{\frac{3}{2}}}\left(\sqrt{u^2+v^2}\right)v + \sigma\beta_0^2 v \tag{3}$$

$$u\frac{\partial T}{\partial x}+v\frac{\partial T}{\partial y}=\alpha_{nf}\left(\frac{\partial^2 T}{\partial x^2}+\frac{\partial^2 T}{\partial y^2}\right) \tag{4}$$

2.1.2 The dimensionless governing equations

The dimensionless variables are:

$$X=\frac{x}{H}, Y=\frac{y}{H}, U=\frac{u}{\epsilon u_o}, V=\frac{v}{\epsilon u_o}, \theta=\frac{T-T_C}{T_H-T_C}, P=\frac{p}{\rho_{nf}u_0^2}, Da=\frac{\kappa}{L^2}, k=\frac{\epsilon^3 d^2}{150(1-\epsilon)^2}, Gr=\frac{g\beta\Delta T L^3}{v_f^2}, Pr=\frac{v_f\rho_f\left(C_p\right)_f}{K_f}, Ra=Gr.Pr, H_a=\beta_0 l\sqrt{\frac{\sigma}{\mu_{nf}}} \tag{5}$$

Eqs. (1)-(4) are reduced as follows after being transformed into dimensionless form:

$$\frac{\partial U}{\partial X}+\frac{\partial V}{\partial Y}=0 \tag{6}$$

$$\frac{1}{\epsilon^2}\left(U\frac{\partial U}{\partial X}+V\frac{\partial U}{\partial Y}\right) = -\frac{\partial P}{\partial X} + \frac{1}{\epsilon}\frac{\rho_f}{\rho_{nf}}\frac{1}{(1-\phi)^{2.5}}\left(\frac{\partial^2 U}{\partial X^2}+\frac{\partial^2 U}{\partial Y^2}\right) - \frac{\mu_{nf}}{\rho_{nf}v_f}\frac{Pr}{Da}U - \frac{1.75}{\sqrt{150Da}\epsilon^{\frac{3}{2}}}\left(\sqrt{U^2+V^2}\right)U \tag{7}$$

$$\frac{1}{\epsilon^2}\left(U\frac{\partial V}{\partial X}+V\frac{\partial V}{\partial Y}\right) = -\frac{\partial P}{\partial Y} + \frac{1}{\epsilon}\frac{\rho_f}{\rho_{nf}}\frac{1}{(1-\phi)^{2.5}}\left(\frac{\partial^2 V}{\partial X^2}+\frac{\partial^2 V}{\partial Y^2}\right) + RaPr\frac{\rho_f}{\rho_{nf}}\left(1-\phi+\frac{\rho_s\beta_s\phi}{\rho_f\beta_f}\right)\theta - \frac{\mu_{nf}}{\rho_{nf}v_f}\frac{Pr}{Da}V - \frac{1.75}{\sqrt{150Da}\epsilon^{\frac{3}{2}}}\left(\sqrt{U^2+V^2}\right)V + PrH_a^2 V \tag{8}$$

$$U\frac{\partial\theta}{\partial X}+V\frac{\partial\theta}{\partial Y}=\frac{1}{Pr}\frac{\alpha_{nf}}{\alpha_f}\frac{k_m}{k_{nf}}\left(\frac{\partial^2\theta}{\partial X^2}+\frac{\partial^2\theta}{\partial Y^2}\right) \tag{9}$$

The boundary conditions are given by:

• Bottom horizontal wall of the cavity is adiabatic (Y=0, X=0 to L)

$$U = 0, V = 0, \frac{\partial \theta}{\partial X} = 0 \tag{10}$$

• Upper horizontal wall is adiabatic (Y=H, X_1= H/tgα to L-X_1)

$$U = 0, V = 0, \frac{\partial \theta}{\partial X} = 0 \tag{11}$$

• The inclined left and right walls

$$U = 0,\ V = 0,\ \theta = 0 \text{ (left)} \tag{12}$$

$$U = 0,\ V = 0,\ \theta = 0 \text{ (right)} \tag{13}$$

• The inner hot rectangular obstacle inside the cavity (Y=0, Y=h)

$$U = 0, V = 0, \theta = 1 \tag{14}$$

2.2 Thermophysical properties of nanofluid

The nanofluid's density, heat capacity, and coefficient of thermal expansion are calculated respectively as follow. Those formulas have been used in numerical simulation of natural convection [40-42].

The diffusion coefficient of nanofluid is presented by:

$$\sigma_{hnf} = (1-\varphi)\sigma_f + \varphi\sigma_{np} \tag{15}$$

The density, the thermal expansion coefficient, the specific heat capacity and the thermal conductivity of nanofluid is given respectively by:

$$\rho_{hnf} = (1-\varphi)\rho_f + \varphi\rho_{np} \tag{16}$$

$$(\rho\beta)_{hnf} = (1-\varphi)(\rho\beta)_f + \varphi(\rho\beta)_{np} \tag{17}$$

$$(\rho c_p)_{hnf} = (1-\varphi)(\rho c_p)_f + \varphi(\rho c_p)_{np} \tag{18}$$

$$\alpha_{hnf} = \frac{k_{hnf}}{(\rho c_p)_{hnf}} \tag{19}$$

$$k_{hnf} = \frac{k_{np} + (n-1)k_f - (n-1)(k_f - k_{np})\varphi}{k_{np} + (n-1)k_f + (k_f - k_{np})\varphi} k_f \tag{20}$$

According to the Brinkman mode, the effective dynamic viscosity is regarded as:

$$\mu_{hnf} = \frac{\mu_f}{(1-\varphi)^{2.5}} \tag{21}$$

Designed for nanoparticles Al_2O_3 and Cu, the properties are obtained [37].

$$\varphi = \varphi Al_2O_3 + \varphi Cu \tag{22}$$

$$\rho_{nf} = \frac{\varphi Al_2O_3(\rho)Al_2O_3 + \varphi Cu(\rho)Cu}{\varphi} \tag{23}$$

$$(C_p)_{nf} = \frac{\varphi Al_2O_3(C_p)Al_2O_3 + \varphi Cu(C_p)Cu}{\varphi} \tag{24}$$

$$\beta_{nf} = \frac{\varphi Al_2O_3(\beta)Al_2O_3 + \varphi Cu(\beta)Cu}{\varphi} \tag{25}$$

$$k_{nf} = \frac{\varphi Al_2O_3(k)Al_2O_3 + \varphi Cu(k)Cu}{\varphi} \tag{26}$$

$$\sigma_{nf} = \frac{\varphi Al_2O_3(\sigma)Al_2O_3 + \varphi Cu(\sigma)Cu}{\varphi} \tag{27}$$

Water base fluid and copper-aluminum oxide nanoparticles, thermo physical properties are presented in Table 1.

Table 1. Thermo-physical properties of the fluid and the nanoparticles (Cu-Al_2O_3/ water (50/50) [43]

Physical Properties	Water	Cu	Al_2O_3
C_p (J/kg k)	4179	383	765
ρ (kg/m^3)	997.1	8954	3600
k (W/m k)	0.6	400	46
$\beta \times 10^{-5}$ (K^{-1})	21	1.67	0.63

2.3 Heat transfer relation

The corresponding average Nusselt numbers are used to express the heat transfer across the hot inner rectangular obstacle.

$$Nu_{local.3} = \frac{k_{nf}}{k_f}\frac{\partial\theta}{\partial Y} \text{ Horizontal wall}$$

$$Nu_{local} = Nu_{local.1} = \frac{k_{nf}}{k_f}\frac{\partial\theta}{\partial X} \text{ Right vertical wall} \tag{28}$$

$$Nu_{local.2} = \frac{k_{nf}}{k_f}\frac{\partial\theta}{\partial X} \text{ Left vertical wall}$$

$$Nu_{average.tot} = \frac{2}{H}\int_0^{H/2} Nu_{local.Right}\, dH + \frac{2}{H}\int_0^{H/2} Nu_{local.Left}\, dH + \frac{7}{L}\int_0^{\frac{L}{7}} Nu_{local.Horizo}\, dL \tag{29}$$

In accordance with Seyyedi et al. [29], the definition of total entropy generation is:

$$Sgen_{Tot} = Sgen_f + Sgen_h \tag{30}$$

Eq. (30), the entropy generated resulting from the flow is denoted by $Sgen_f$, while the entropy generated caused by heat is represented by $Sgen_h$.

$$Sgen_f = \frac{k_{nf}}{\theta_0^2}\left[\left(\frac{\partial\theta}{\partial X}\right)^2 + \left(\frac{\partial\theta}{\partial Y}\right)^2\right] \tag{31}$$

$$Sgen_h = \frac{k_{nf}}{\theta_0}\left[2\left(\frac{\partial U}{\partial X}\right)^2 + 2\left(\frac{\partial V}{\partial Y}\right)^2 + \left(\frac{\partial U}{\partial X} + \frac{\partial V}{\partial Y}\right)\right] + \frac{\sigma_{nf}}{\sigma}Ha^2V^2 \text{ and } \theta_0 = \frac{\theta_c + \theta_h}{2} \tag{32}$$

2.4 Validation

Numerical results published in the literature were used to validate the computer code. The dimensionless temperature in the cavity's midplane (Y=0.5) is compared to the benchmark study of Khanafer et al. [15] (Figure 2).

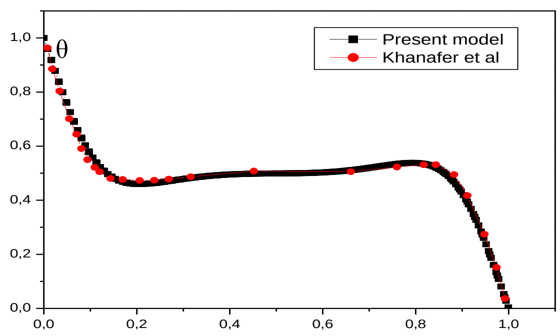

Figure 2. The comparison of dimensionless temperature for ϕ=0.01, Pr=6.8, and Ra=6.8.10^4 at the midplane (Y=0.5)

3. RESULTS AND DISCUSSION

These results present the alteration of streamlines (ψ), isotherms (θ), the average Nusselt numbers (Nu_{avg}), and entropy generation (S) for various values of impacted parameters like Rayleigh number Ra (Ra =10^2 ,10^3 ,10^5), Hartman number Ha (Ha=0, 100) and varying position of hot rectangular barrier (0.5, 0.9, 1.9) for fixed Darcy number Da=10^{-1}, proportion of nanoparticles in volume ϕ=0.02 and porosity ϵ=0.5 through contours as observed in Figures 3-10.

3.1 Effects of Rayleigh number (Ra) on (ψ), (θ) and (S)

Figure 3 presents the variation of streamlines, isotherms and entropy generation for varying Ra at Ha=0.0 and Da=10^{-1}.

As Ra=10^3, the thermal buoyancy-driven convection is very feeble, we observe a horizontal stratification of the isotherms due to the stagnant fluid in the center of the enclosure. The streamlines form two single cells turning in the clockwise and unclockwise direction respectively. The heat transfer exhibits the characteristics of pure conduction. The overall shape of the streamlines demonstrates a downward flow at the cold inclined sides and an upward flow at the inner heated rectangular barrier for Ra≥10^5.

For further, we observe that the variation of Ra number affects significantly the entropy generation because of a large temperature differential between the nanofluid and the hot and cold walls respectively. The entropy (S) is important in the vicinity of active walls.

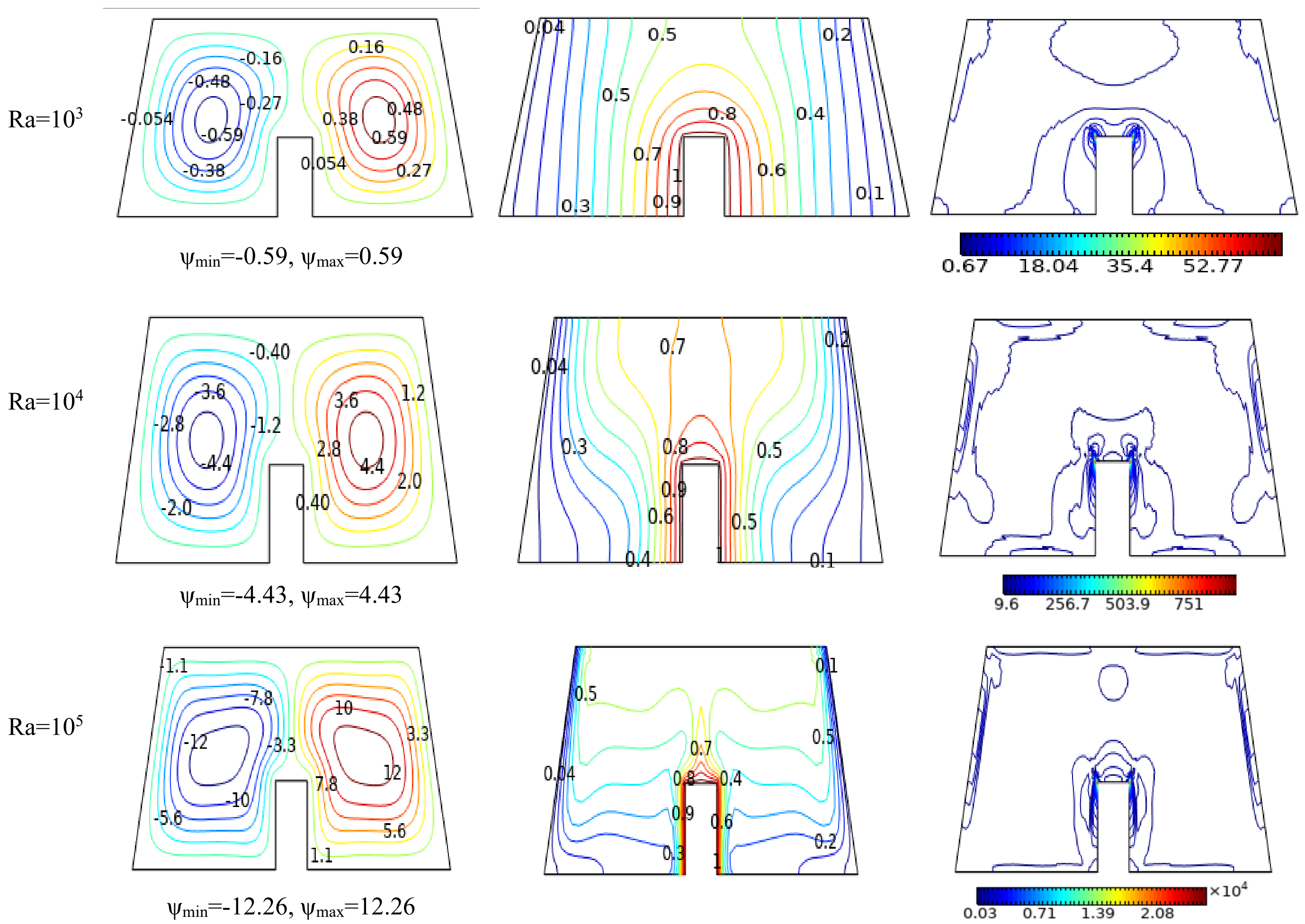

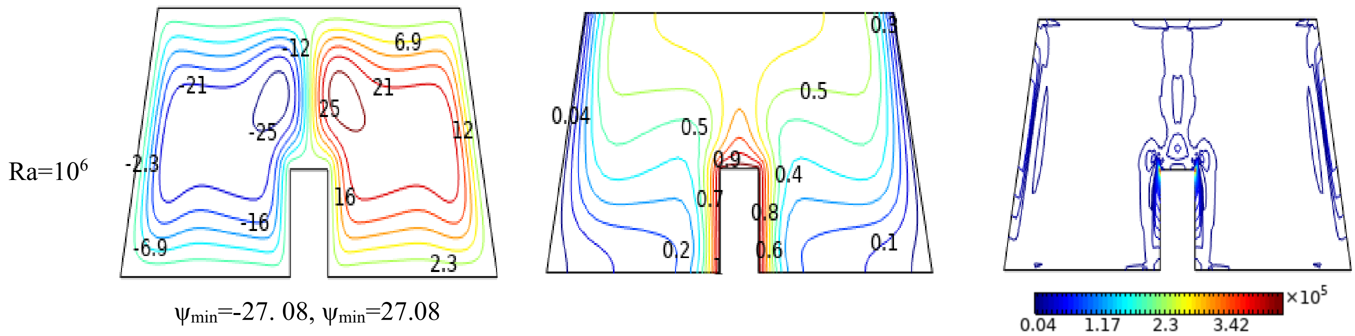

Figure 3. The variation of (ψ), (θ) and (S) for different Ra at ϕ=0.02, ϵ=0.5, Da=10^{-1} and Ha=0

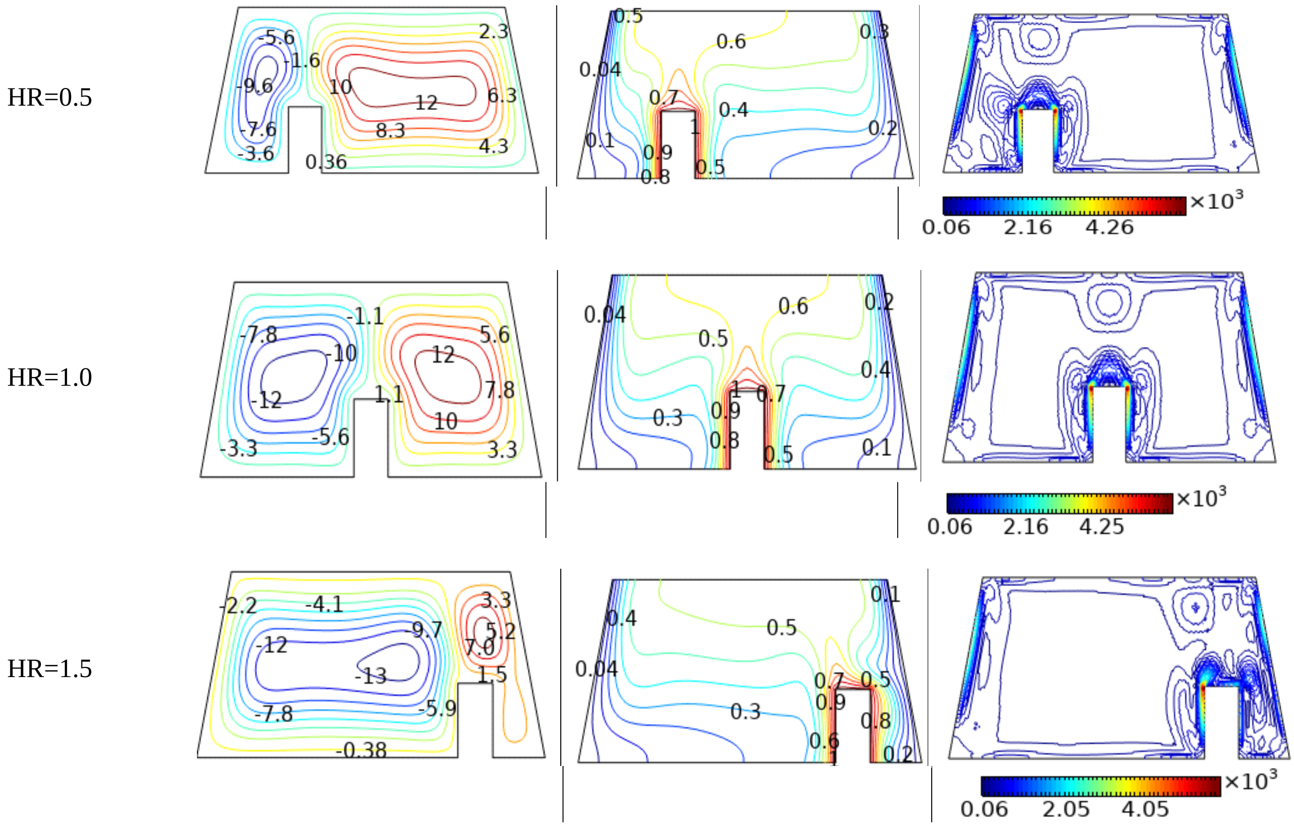

Figure 4. The plot of the (ψ), (θ) and (S) for different a) HR=0.5, b) HR=1.0 and c) HR=1.5 at ϕ=0.02, ϵ=0.5, Da=10^{-1} and Ha=0

3.2 Effects of location inner hot rectangular barrier (HR) on (ψ), (θ) and (S)

To highlight the effect of the location of the hot barrier (HR), we have considered different positions HR=0.5, 1 and 1.5 for fixed Ra=10^5. By observing the isotherms in Figure 4, when HR=1.0, we see that the heat flow is horizontal, through the thermal boundary layers at vicinity of actives walls (hot and cold walls), then it becomes vertical descending through vertical stratification gradually as we approach the middle space of the cavity with a low temperature gradient. On the other hand, when the position of the hot barrier is HR=0.5 and HR=1.5 Figure 4(a) and Figure 4(c), The fluid heats up more efficiently when the hot barrier is close to the cold wall. The temperature gradient is extremely strong at the hot wall and weak at the cold wall (HR=0.5, 1.5). The entropy (S) is considerable when the hot barrier is close to the cold wall (HR=0.5, 1.5). These results suggest that hot barriers can enhance thermal performance, which has significant implications for thermal system design.

3.3 Effects of Hartman number (Ha) on (ψ), (θ) and (S)

Figure 5 presents the development of (θ), (ψ) and entropy (S) inside the enclosure. The (θ) and (ψ) under a magnetic field demonstrate that the increasing of (Ha) number reduces the stream values. Figure 5(a) illustrates how the stream value decreases by 78% for Ha=0 to Ha=25 and by 230% for Ha=0 to Ha=100. Based on these findings, we can conclude that the magnetic induction intensity limits the fluid's mobility.

Furthermore, as the fluid becomes immobile in the cavity, the thermal exchange is significantly decreases. The entropy (S) is exclusively surrounding the heated obstacle, the isothermal contours is illustrated by horizontal stratification. The Entropy (S) is presented in Figure 5(c) where the (Ha) number is varied from 0 to 100. The thermal entropy decreases by around 69% as the (Ha) number increases for 0 to 25, but it decreases by 356% when Ha is increased from 25 to 50. By carefully modifying the (Ha) number, heat transfer efficiency can be managed.

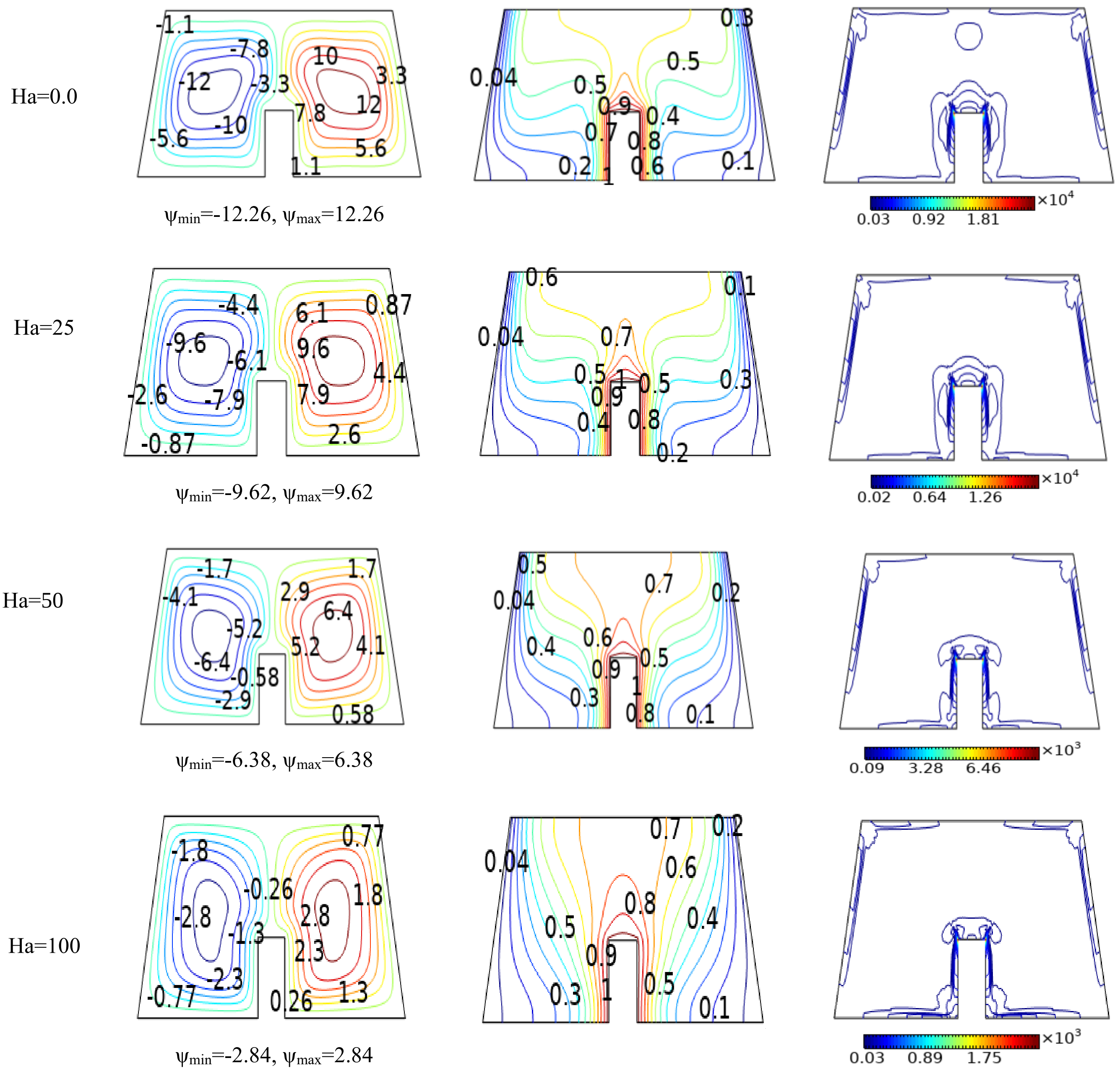

Figure 5. The variation of the (ψ), (θ) and (S) for different Ha at ϕ=0.02, ϵ=0.5, Da=10^{-1}

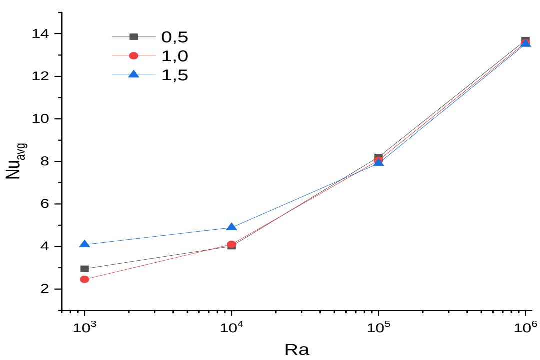

Figure 6. The Nu_{avg} number for different (Ra) number and location of inner hot barrier (HR) at ϕ=0.02, ϵ=0.5, Da=10^{-1} and Ha=25

3.4 Effects of location inner hot rectangular barrier (HR) on main (Nu) number

Figure 6 provides the trend of (Nu) for various (Ra) number and various location of inner hot barrier (HR). The results illustrate that the increasing the Ra number is proportional to increasing of heat transfer for all position of hot barrier HR. Also, for low Ra number in range 10^3, 10^4 the heat transfer is important for HR=1.5 compared with the authors cases HR=0.5 and HR=1.0, because of the impact of a magnetic field applied in left side of the cavity. The heat exchange is favorable in the narrow space between the hot and cold walls. The system design implications are noteworthy, indicating that thermal management can be significantly enhanced by moving the hot barrier.

3.5 Effects of (Ha) on the Nu_{avg} number

Figure 7 shows how the Hartmann number affects the (Nu) number; as the (Ha) number rises, the Nu number falls. The magnetic fields can be used to control fluid motion, but they may also decrease the efficiency of heat transfer. This has important consequences for system design. Therefore, it is crucial to evaluate the usage of magnetic fields in thermal management systems to strike a balance between fluid movement and heat transfer performance.

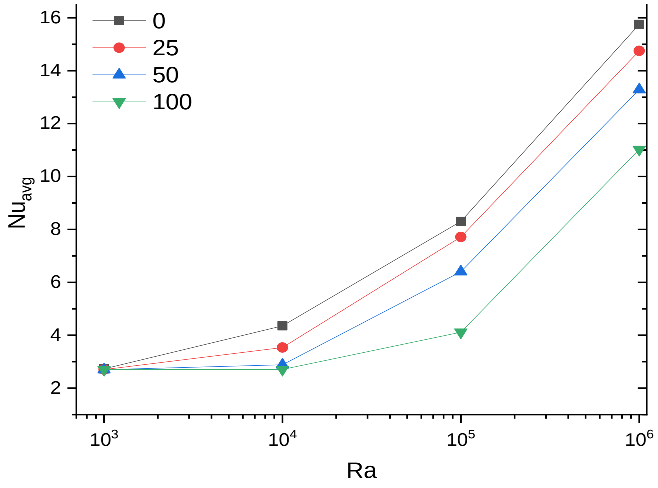

Figure 7. The main (Nu) number for various (Ha) number and different (Ra) number at ϕ=0.02, ϵ=0.5, Da=10^{-1} and HR=1.0

3.6 Impact of porosity (ϵ) on the Nu_{avg} number

Figure 8 presents the influence of porosity on the (Nu_{avg}) number for various volume fractions (ϕ) at (Da) number of 10^{-2}, Ha=0, and Ra=10^5. The results show that increasing porosity is proportional to the average Nusselt number. As porosity is important (ϵ=0.5), the hybrid nanofluid move freely through the orifices of the porous medium, thereby enhancing heat transfer.

Furthermore, the heat exchange capacity is enhanced by the volume fraction (ϕ) due to the increasing of thermal conductivity. The Nu_{avg} number for ϕ=0.06 is 5% higher than ϕ=0.02.

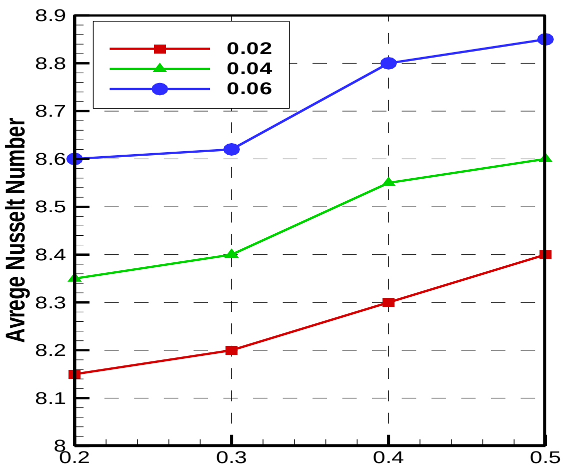

Figure 8. The Nu_{avg} number for various (ϵ) and different volumes fractions (ϕ) at Ra=10^5, Ha=0.0, Da=10^{-2} and HR=1.0

3.7 Impact of Hartman number (Ha) on the Nu_{avg} number

Figures 9 indicates the evolution of the (Nu_{avg}) number induced by the (Ha) number. The (Nu_{avg}) number and the Hartmann number are shown to be inversely related. As the Hartmann number increases to 25 and 100, it significantly impacts heat transfer by reducing the Nusselt number for all volume fractions ranging from 2% to 6%.

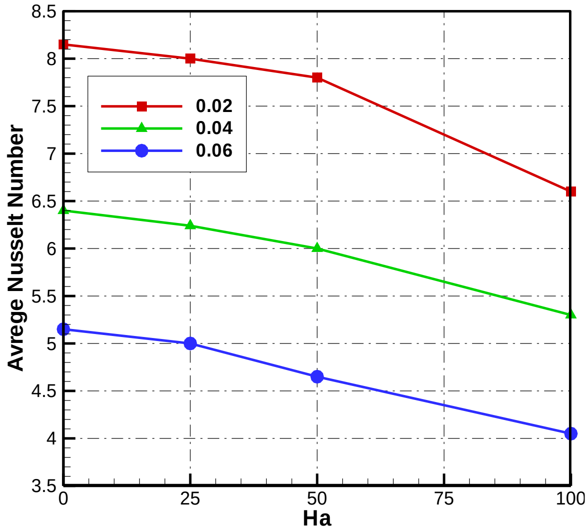

Figure 9. The Nu_{avg} number for differents (Ha) and volumes fractions (ϕ) at Ra=10^5, ϵ=0.5, Da=10^{-2} and HR=1.0

Magnetic fields can be used to control fluid motion, but they may also decrease the efficiency of heat transfer. This has important consequences for system design. The use of magnetic fields in thermal systems must therefore be carefully considered in order to balance the relation-ship between heat transfer performance and fluid motion control.

3.8 Impact of Hartman number (Ha) on total entropy generation (S_{Tot})

The variations of (S_{Tot}) for different parameters are shown in Figure 10, including the volume fraction of the hybrid nanofluid and high values of (Da) number. According to the plot. 11, the entropy is enhanced when the volume fraction (ϕ) increases, particularly at high volume fractions (ϕ=6%) and significant porosity (ϵ=0.5). According to quantitative measurements, the entropy (S_{Tot}) at ϕ=6% and ϵ=0.5 is substantially higher than at lower volume fractions.

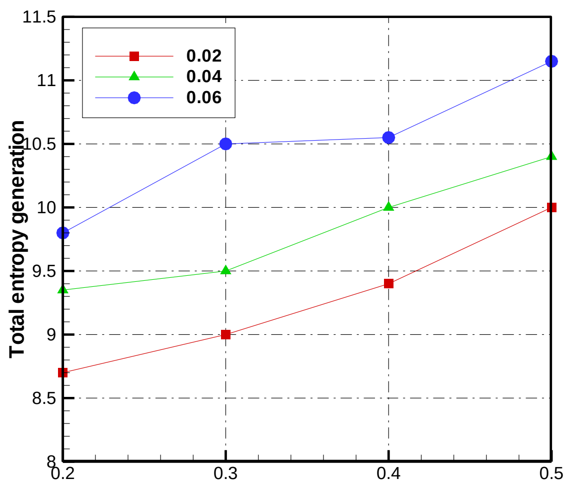

Figure 10. The total entropy (S_{Tot}) for various (ϵ) and different volumes fractions (ϕ) at Ra=10^5, Ha=0.0, Da=10^{-2} and HR=1.0

4. CONCLUSION

Entropy generation study of magnetohydrodynamic convection, two-dimensional laminar Hybrid nanofluid flow inside a trapezoidal cavity with hot inner rectangular barrier was carried out. These flows have numerous technical uses, which makes them extremely important. The effects of Ra, Ha and HR on isotherms, streamline and entropy generation were examined. Results indicated that:

1) Heat transfer is enhanced when the Ra number increase, whereas it decreases when the Ha number increase.
2) For low Ra values, the heat exchange was more substantial for HR=1.5 than other position HR=0.5 and HR=1.0.
3) Entropy generation increase as Ra number increased but it decreases when Ha number increased.
4) Heat transfer was enhanced by the hybrid nanofluid's volume fraction. The Nu_{avg} number for ϕ=0.06 is 5% higher than ϕ=0.02.
5) The isotherms, streamlines, and entropy generation were all strongly impacted by the displacement of the inner hot barrier.
6) To enhance heat transfer and entropy generation in porous media systems, it is recommended to optimize these parameters, (Ra), (Ha) and (ϕ).

REFERENCE

[1] De Mey, G., Torzewicz, T., Kawka, P., Czerwoniec, A., Janicki, M., Napieralski, A. (2016). Analysis of nonlinear heat exchange phenomena in natural convection cooled electronic systems. Microelectronics Reliability, 67: 15-20. https://doi.org/10.1016/j.microrel.2016.11.003

[2] Purusothaman, A. (2018). Investigation of natural convection heat transfer performance of the QFN-PCB electronic module by using nanofluid for power electronics cooling applications. Advanced Powder Technology, 29(4): 996-1004. https://doi.org/10.1016/j.apt.2018.01.018

[3] Liang, M., Liu, Y., Xiao, B., Yang, S., Wang, Z., Han, H. (2018). An analytical model for the transverse permeability of gas diffusion layer with electrical double layer effects in proton exchange membrane fuel cells. International Journal of Hydrogen Energy, 43(37): 17880-17888. https://doi.org/10.1016/j.ijhydene.2018.07.186

[4] Shafieian, A., Khiadani, M., Nosrati, A. (2018). A review of latest developments, progress, and applications of heat pipe solar collectors. Renewable and Sustainable Energy Reviews, 95: 273-304. https://doi.org/10.1016/j.rser.2018.07.014

[5] Phiraphat, S., Prommas, R., Puangsombut, W. (2017). Experimental study of natural convection in PV roof solar collector. International Communications in Heat and Mass Transfer, 89: 31-38. https://doi.org/10.1016/j.icheatmasstransfer.2017.09.022

[6] Wang, F.Z., Sohail, M., Nazir, U., Awwad, E.M., Sharaf, M. (2024). Utilization of the Crank-Nicolson technique to investigate thermal enhancement in 3D convective Walter-B fluid by inserting tiny nanoparticles on a circular cylinder. AIMS Mathematics, 9(4): 9059-9090. https://doi.org/10.3934/math.2024441

[7] Ali, S., Shaiq, S., Shahzad, A., Sohail, M., Naseem, T. (2024). Numerical thermal investigation of radiative magnetohydrodynamics axisymmetric Cu-Al_2O_3/H_2O hybrid nanofluid flow over an unsteady radially stretched surface. International Journal of Ambient Energy, 45(1): 2321210. https://doi.org/10.1080/01430750.2024.2321210

[8] Reddy, N.K., Swamy, H.K., Sankar, M., Jang, B. (2023). MHD convective flow of Ag-TiO_2 hybrid nanofluid in an inclined porous annulus with internal heat generation. Case Studies in Thermal Engineering, 42: 102719. https://doi.org/10.1016/j.csite.2023.102719

[9] Swamy, H.K., Reddy, N.K., Sankar, M., Peddinti, P.R. (2023). Conjugate heat transfer of aqueous hybrid nanoliquid between coaxial cylinders subjected to magnetic field. International Journal of Thermofluids, 17: 100299. https://doi.org/10.1016/j.ijft.2023.100299

[10] Mebarek-Oudina, F., Chabani, I., Vaidya, H., Ismail, A. A.I. (2024). Hybrid-nanofluid magneto-convective flow and porous media contribution to entropy generation. International Journal of Numerical Methods for Heat & Fluid Flow, 34(2): 809-836. https://doi.org/10.1108/HFF-06-2023-0326

[11] Esfe, M.H., Rostamian, H., Toghraie, D., Hekmatifar, M., Abad, A.T.K. (2022). Numerical study of heat transfer of U-shaped enclosure containing nanofluids in a porous medium using two-phase mixture method. Case Studies in Thermal Engineering, 38: 102150. https://doi.org/10.1016/j.csite.2022.102150

[12] Ali, F.H., Hamzah, H.K., Egab, K., Arıcı, M., Shahsavar, A. (2020). Non-Newtonian nanofluid natural convection in a U-shaped cavity under magnetic field. International Journal of Mechanical Sciences, 186: 105887. https://doi.org/10.1016/j.ijmecsci.2020.105887

[13] Nabwey, H.A., Rashad, A.M., Khan, W.A., Alshber, S.I. (2022). Effectiveness of magnetize flow on nanofluid via unsteady natural convection inside an inclined U-shaped cavity with discrete heating. Alexandria Engineering Journal, 61(11): 8653-8666. https://doi.org/10.1016/j.aej.2022.02.010

[14] Choi, S.U.S., Eastman, J.A. (1995). Enhancing thermal conductivity of fluids with nanoparticles. In Proceedings of the ASME International Mechanical Engineering Congress & Exposition, San Francisco, CA, USA, pp. 12-17.

[15] Khanafer, K., Vafai, K., Lightstone, M. (2003). Buoyancy-driven heat transfer enhancement in a two-dimensional enclosure utilizing nanofluids. International Journal of Heat and Mass Transfer, 46(19): 3639-3653. https://doi.org/10.1016/S0017-9310(03)00156-X

[16] Khanafer, K., Vafai, K. (2017). A critical synthesis of thermophysical characteristics of nanofluids. International Journal of Heat and Mass Transfer, 54(19-20): 4410-4428. https://doi.org/10.1016/j.ijheatmasstransfer.2011.04.048

[17] Boungioron, J. (2006). Convective transport in nanofluids. ASME Journal of Heat and Mass Transfer. 128(3): 240-250. https://doi.org/10.1115/1.2150834

[18] Kefayati, G.H.R. (2016). Heat transfer and entropy generation of natural convection on non-Newtonian nanofluids in a porous cavity. Powder Technology, 299: 127-149. https://doi.org/10.1016/j.powtec.2016.05.032

[19] Al-Kouz, W., Alshare, A., Kiwan, S., Al-Muhtady, A., Alkhalidi, A., Saadeh, H. (2018). Two-dimensional analysis of low-pressure flows in an inclined square cavity with two fins attached to the hot wall. International Journal of Thermal Sciences, 126: 181-193. https://doi.org/10.1016/j.ijthermalsci.2018.01.005

[20] Ghasemi, B., Aminossadati, S.M., Raisi, A. (2011). Magnetic field effect on natural convection in a nanofluid-filled square enclosure. International Journal of Thermal Sciences, 50(9): 1748-1756. https://doi.org/10.1016/j.ijthermalsci.2011.04.010

[21] Kefayati, G.R., Hosseinizadeh, S.F., Gorji, M., Sajjadi, H. (2011). Lattice Boltzmann simulation of natural convection in tall enclosures using water/SiO_2 nanofluid. International Communications in Heat and Mass Transfer, 38(6): 798-805. https://doi.org/10.1016/j.icheatmasstransfer.2011.03.005

[22] Al-Kouz, W.G., Kiwan, S., Alkhalidi, A., Sari, M.E., Alshare, A. (2018). Numerical study of heat transfer enhancement for low-pressure flows in a square cavity with two fins attached to the hot wall using Al_2O_3-Air nanofluid. Strojniški Vestnik-Journal of Mechanical Engineering, 64(1): 26-36. https://doi.org/10.5545/sv-jme.2017.4989

[23] Nield, D.A. (1991). The limitations of the Brinkman-Forchheimer equation in modeling flow in a saturated porous medium and at an interface. International Journal of Heat and Fluid Flow, 12(3): 269-272. https://doi.org/10.1016/0142-727X(91)90062-Z

[24] Asim, M., Siddiqui, F.R. (2022). Hybrid nanofluids-next-generation fluids for spray-cooling-based thermal management of high-heat-Flux devices. Nanomaterials, 12(3): 507. https://doi.org/10.3390/nano12030507

[25] Gao, J., Liu, J., Yue, H., Zhao, Y., Tlili, I., Karimipour, A. (2022). RETRACTED: Effects of various temperature and pressure initial conditions to predict the thermal conductivity and phase alteration duration of water based carbon hybrid nanofluids via MD approach. Journal of Molecular Liquids, 351: 118654. https://doi.org/10.1016/j.molliq.2022.118654

[26] Wohld, J., Beck, J., Inman, K., Palmer, M., Cummings, M., Fulmer, R., Vafaei, S. (2022). Hybrid nanofluid thermal conductivity and optimization: Original approach and background. Nanomaterials, 12(16): 2847. https://doi.org/10.3390/nano12162847

[27] Mebarek-Oudina, F.P.A.S., Preeti, Sabu, A.S., Vaidya, H., Lewis, R.W., Areekara, S., Mathew, A., Ismail, A.I. (2024). Hydromagnetic flow of magnetite-water nanofluid utilizing adapted Buongiorno model. International Journal of Modern Physics B, 38(01): 2450003. https://doi.org/10.1142/S0217979224500036

[28] Kleinstreuer, C., Feng, Y. (2011). Experimental and theoretical studies of nanofluid thermal conductivity enhancement: A review. Nanoscale Research Letters, 6: 229. https://doi.org/10.1186/1556-276X-6-229

[29] Seyyedi, S.M. (2020). On the entropy generation for a porous enclosure subject to a magnetic field: Different orientations of cardioid geometry. International Communications in Heat and Mass Transfer, 116: 104712. https://doi.org/10.1016/j.icheatmasstransfer.2020.104712

[30] Acharya, N., Mabood, F., Shahzad, S.A., Badruddin, I.A. (2022). Hydrothermal variations of radiative nanofluid flow by the influence of nanoparticles diameter and nanolayer. International Communications in Heat and Mass Transfer, 130: 105781. https://doi.org/10.1016/j.icheatmasstransfer.2021.105781

[31] Subhani, M., Nadeem, S. (2019). Numerical investigation into unsteady magnetohydrodynamics flow of micropolar hybrid nanofluid in porous medium. Physica Scripta, 94(10): 105220. https://doi.org/10.1088/1402-4896/ab154a

[32] Chabani, I., Mebarek-Oudina, F., Vaidya, H., Ismail, A.I. (2022). Numerical analysis of magnetic hybrid nano-fluid natural convective flow in an adjusted porous trapezoidal enclosure. Journal of Magnetism and Magnetic Materials, 564: 170142. https://doi.org/10.1016/j.jmmm.2022.170142

[33] Marzougui, S., Mebarek-Oudina, F., Magherbi, M., Mchirgui, A. (2021). Entropy generation and heat transport of Cu-water nanoliquid in porous lid-driven cavity through magnetic field. International Journal of Numerical Methods for Heat & Fluid Flow, 32(6): 2047-2069. https://doi.org/10.1108/HFF-04-2021-0288

[34] Nayak, M.K., Mabood, F., Dogonchi, A.S., Ramadan, K.M., Tlili, I., Khan, W.A. (2025). Entropy optimized assisting and opposing non-linear radiative flow of hybrid nanofluid. Waves in Random and Complex Media, 35(1): 1389-1410. https://doi.org/10.1080/17455030.2022.2032474

[35] Sheikholeslami, M., Abohamzeh, E., Ebrahimpour, Z., Said, Z. (2022). Brief overview of the applications of hybrid nanofluids. Hybrid Nanofluids, 171-202. https://doi.org/10.1016/B978-0-323-85836-6.00008-9

[36] Nazir, U., Sohail, M., Kumam, P., Elmasry, Y., Sitthithakerngkiet, K., Ali, M.R., Khan, M.J., Galal, A.M. (2022). Thermal and solute aspects among two viscosity models in synovial fluid inserting suspension of tri and hybrid nanomaterial using finite element procedure. Scientific Reports, 12(1): 21577. https://doi.org/10.1038/s41598-022-23271-0

[37] Alsabery, A.I., Kadhim, H.T., Ismael, M.A., Hashim, I., Chamkha, A.J. (2023). Impacts of amplitude and heat source on natural convection of hybrid nanofluids into a wavy enclosure via heatline approach. Waves in Random and Complex Media, 33(4): 1060-1084. https://doi.org/10.1080/17455030.2021.1896819

[38] Nguyen, M.T., Aly, A.M., Lee, S.W. (2015). Natural convection in a non-darcy porous cavity filled with Cu-water nanofluid using the characteristic-based split procedure in finite-element method. Numerical Heat Transfer, Part A: Applications, 67(2): 224-247. https://doi.org/10.1080/10407782.2014.923225

[39] Bourantas, G.C., Skouras, E.D., Loukopoulos, V.C., Burganos, V.N. (2014). Heat transfer and natural convection of nanofluids in porous media. European Journal of Mechanics-B/Fluids, 43: 45-56. https://doi.org/10.1016/j.euromechflu.2013.06.013

[40] Jou, R.Y., Tzeng, S.C. (2006). Numerical research of nature convective heat transfer enhancement filled with nanofluids in rectangular enclosures. International Communications in Heat and Mass Transfer, 33(6): 727-736. https://doi.org/10.1016/j.icheatmasstransfer.2006.02.016

[41] Oztop, H.F., Abu-Nada, E. (2008). Numerical study of natural convection in partially heated rectangular enclosures filled with nanofluids. International Journal of Heat and Fluid Flow, 29(5): 1326-1336. https://doi.org/10.1016/j.ijheatfluidflow.2008.04.009

[42] Pordanjani, A.H., Vahedi, S.M., Rikhtegar, F., Wongwises, S. (2019). Optimization and sensitivity analysis of magneto-hydrodynamic natural convection nanofluid flow inside a square enclosure using response surface methodology. Journal of Thermal Analysis and Calorimetry, 135: 1031-1045. https://doi.org/10.1007/s10973-018-7652-6

[43] Mehryan, S.A., Kashkooli, F.M., Ghalambaz, M., Chamkha, A.J. (2017). Free convection of hybrid Al_2O_3-Cu water nanofluid in a differentially heated porous cavity. Advanced Powder Technology, 28(9): 2295-2305. https://doi.org/10.1016/j.apt.2017.06.011